

Exploring Active Learning in Meta-Learning: Enhancing Context Set Labeling

Wonho Bae¹, Jing Wang¹, and Danica J. Sutherland^{1,2}

¹ University of British Columbia, Vancouver

² Alberta Machine Intelligence Institute (Amii)

whbae@cs.ubc.ca, jing@ece.ubc.ca, dsuth@cs.ubc.ca

Abstract. Most meta-learning methods assume that the (very small) context set used to establish a new task at test time is passively provided. In some settings, however, it is feasible to actively select which points to label; the potential gain from a careful choice is substantial, but the setting requires major differences from typical active learning setups. We clarify the ways in which active meta-learning can be used to label a context set, depending on which parts of the meta-learning process use active learning. Within this framework, we propose a natural algorithm based on fitting Gaussian mixtures for selecting which points to label; though simple, the algorithm also has theoretical motivation. The proposed algorithm outperforms state-of-the-art active learning methods when used with various meta-learning algorithms across several benchmark datasets.

Keywords: Meta learning · Active learning · Low budget

1 Introduction

Meta-learning has gained significant prominence as a substitute for traditional “plain” supervised learning tasks, with the aim to adapt or generalize to new tasks given extremely limited data. (Hospedales *et al.* [30] give a recent survey.) There has been enormous success compared to learning “from scratch” on each new problem, but could we do even better, with even less data?

One major way to improve data-efficiency in standard supervised learning settings is to move to an *active* learning paradigm, where typically a model can request a small number of labels from a pool of unlabeled data; these are collected, used to further train the model, and the process is repeated. (Settles *et al.* [59] provides a classic overview, and Ren *et al.* [54] a more recent survey.)

Although each of these lines of research are well-developed, their combination – *active meta-learning* – has seen comparatively little research attention. This intersection, however, is not only theoretically appealing but also has numerous practical applications. For example, in medical imaging, there is often a large repository of labeled X-ray or MRI images. However, labeling these images requires manual annotations by radiologists or pathologists, which is time-consuming and costly. In manufacturing, there is often a large amount of sensor

data generated during the production process. Annotating them to identify patterns indicating quality issues requires domain experts.

How can a meta-learner leverage an active learning setup to learn the best model possible, using only a few labels in its context sets? We are aware of three previous attempts at active selection of context sets in meta-learning: Müller *et al.* [43] and Al-Shedivat *et al.* [3] do so at meta-*training* time for text and image classification, while Boney *et al.* [9] do it at meta-*test* time in semi-supervised few-shot image classification with ProtoNet [61]. “Active meta-learning” thus means very different things in their procedures; these approaches are also entirely different from work on active selection of *tasks* during meta-training [32, 37, 47]. Our first contribution is therefore to clarify the different ways in which active learning can be applied to meta-learning, for differing purposes.³

We then confirm in extensive experiments that no active learning method for context set selection seems to significantly help with final predictor quality at meta-training time – aligning with previous observations by Setlur *et al.* [58] and Ni *et al.* [46] – but that active learning *can* substantially help at meta-test time. In particular, we propose a natural algorithm based on fitting a Gaussian mixture model to the unlabeled data, using meta-learned feature representations; though the approach is simple, we also give theoretical motivation. We show that our proposed selection algorithm works reliably, and often substantially outperforms competitor methods across many different meta-learning and few-shot learning tasks, across a variety of benchmark datasets and meta-learning algorithms. Our contributions are summarized as follows.

- We explore the concept of “active meta-learning,” pointing out that active selection can occur in several places (Sec. 2) and highlighting challenges in traditional meta-learning setups regarding sample stratification (Sec. 2.1).
- We identify that existing active learning algorithms, particularly low-budget active learning methods, perform poorly in active meta-learning (Sec. 4), even if meta-learning is in the low-budget regime.
- We propose a method based on Gaussian mixture model using meta-learning specific features (Sec. 3.2), proven to yield a Bayes-optimal classifier under certain assumptions (or an efficient set cover in a general setting in Sec. 3.3).
- Our experiments show that the simple Gaussian mixture method consistently outperforms more complex active learning methods across various few-shot image classification (Secs. 4.1 and 4.2), cross-domain classification (Sec. 4.3), and meta-learning regression tasks (Sec. 4.4), irrespective of the type of meta-learning algorithms employed.

2 Meta-Learning: Background and Where to be “Active”

We aim to learn a learning algorithm f_θ , a function which, given a dataset \mathcal{C} consisting of pairs $(x, y) \in \mathcal{X} \times \mathcal{Y}$, returns $g := f_\theta(\mathcal{C})$. The function $g : \mathcal{X} \rightarrow \mathcal{Y}$ is

³ Note that work on meta-learning an active selection criterion for higher-label-budget problems – *e.g.* [16, 36] – is essentially unrelated.

a classifier, regressor, or so on. We evaluate the quality of g using a loss function $\ell : \hat{\mathcal{Y}} \times \mathcal{Y} \rightarrow \mathbb{R}$, e.g. the cross-entropy or square loss:

$$\text{Empirical risk of } g \text{ on } \mathcal{T}: \mathcal{R}_\ell(g, \mathcal{T}) = \frac{1}{|\mathcal{T}|} \sum_{(x,y) \in \mathcal{T}} \ell(g(x), y).$$

To find the θ which gives the best g s, we assume we have access to distributions $\mathcal{P}^{train}, \mathcal{P}^{eval}$ over tasks $\mathcal{D} \subseteq \mathcal{X} \times \mathcal{Y}$. For each task, we will run f_θ on a *context set* \mathcal{C} , then evaluate the quality of the learned predictor on a disjoint *target set* \mathcal{T} . We call the distribution over possible $(\mathcal{C}, \mathcal{T})$ pairs $\text{Pick}_\theta(\mathcal{D})$.⁴ For instance, the default choice in passive meta-learning chooses, say, five random points per class for \mathcal{C} and assigns the rest to \mathcal{T} , ignoring θ and x . Our aim is then,

Meta-training: find $\hat{\theta}$ using

$$\hat{\theta} \approx \arg \min_{\theta} \mathbb{E}_{\mathcal{D} \sim \mathcal{P}^{train}} \left[\mathbb{E}_{(\mathcal{C}, \mathcal{T}) \sim \text{Pick}_\theta^{train}(\mathcal{D})} \left[\mathcal{R}_{\ell^{train}}(f_\theta(\mathcal{C}), \mathcal{T}) \right] \right]. \quad (1)$$

Many algorithms have been proposed for meta-training (overviewed in Sec. 2.2).

To compare models based on \mathcal{P}^{eval} , we might evaluate with a different loss. For instance, it would be typical to use the 0-1 loss (corresponding to accuracy) for classification problems, despite training with cross-entropy.

$$\text{Meta-testing: eval. } f_{\hat{\theta}} \text{ using } \mathbb{E}_{\tilde{\mathcal{D}} \sim \mathcal{P}^{eval}} \left[\mathbb{E}_{(\tilde{\mathcal{C}}, \tilde{\mathcal{T}}) \sim \text{Pick}_{\hat{\theta}}^{eval}(\tilde{\mathcal{D}})} \left[\mathcal{R}_{\ell^{eval}}(f_{\hat{\theta}}(\tilde{\mathcal{C}}), \tilde{\mathcal{T}}) \right] \right]. \quad (2)$$

Finally, in practice, we might want to use a different selection scheme at deployment time. For instance, in passive meta-learning, one would typically use all available labeled data for context, not a random subset. Given a task $\check{\mathcal{D}}$,

$$\text{Deployment: find a context set via } (\check{\mathcal{C}}, _) \sim \text{Pick}_{\hat{\theta}}^{deploy}(\check{\mathcal{D}}) \text{ and use } f_{\hat{\theta}}(\check{\mathcal{C}}). \quad (3)$$

2.1 Active Selection of Context in Meta Learning

There are several places where active learning can be applied during meta-learning. In the meta-training phase (1), we could actively choose tasks \mathcal{D} , and/or have $\text{Pick}_\theta^{train}$ actively select points for \mathcal{C} and/or \mathcal{T} . At meta-testing time (2), we could have $\text{Pick}_\theta^{eval}$ actively select points for $\tilde{\mathcal{C}}$ and/or $\tilde{\mathcal{T}}$; we might also actively choose $\tilde{\mathcal{D}}$ to use labels efficiently, similarly to active surveying [22]. At deployment time (3), $\text{Pick}_\theta^{deploy}$ might actively choose a context set $\check{\mathcal{C}}$ to label.

Actively selecting \mathcal{D} , $\tilde{\mathcal{D}}$, \mathcal{T} , and/or $\tilde{\mathcal{T}}$ is interesting to minimize the label burden (or, possibly, computational cost) of meta-training [32, 37, 47]. We assume here, however, that \mathcal{P}^{train} and \mathcal{P}^{eval} are based on already-labeled datasets.

⁴ If we pick points by some deterministic process, $\text{Pick}_\theta(\mathcal{D})$ is a point mass.

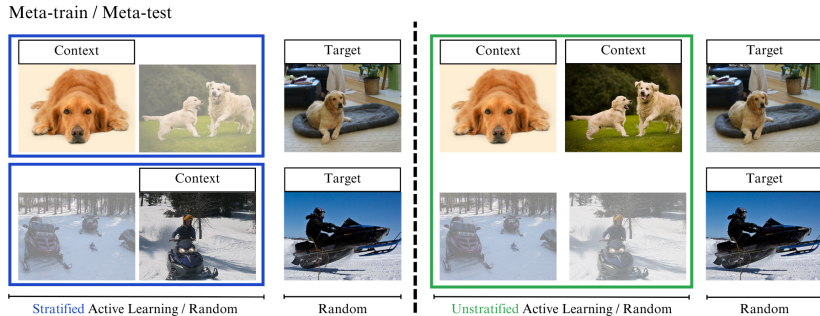


Fig. 1: Meta-training process. Pick_θ can be stratified or unstratified, active or passive.

Instead, we are primarily concerned with the labeling burden at deployment time, and so our final goal is to actively select $\tilde{\mathcal{C}}$ with $\text{Pick}_\theta^{\text{deploy}}$ to find the best predictor. To evaluate how well we should expect our algorithms to perform at this task, we choose $\text{Pick}_\theta^{\text{eval}} = \text{Pick}_\theta^{\text{deploy}}$; thus, we actively select $\tilde{\mathcal{C}}$.

Should we expect this to help? Efficient approaches for data selection in meta-learning have not yet received much research attention. Setlur *et al.* [58] suggest that context set diversity is empirically not particularly helpful for meta-learning, and Ni *et al.* [46] show that data augmentation on context sets is not very useful either. Pezeshkpour *et al.* [50] further provide some evidence using label information that there is not much room to improve few-shot classification with active learning. Agarwal *et al.* [1], however, argue against these previous findings, showing that adversarially selected context sets, at both training and test time, significantly change the classification performance. Their approach is not applicable in practice since it requires full label information, but may suggest there is room to improve meta-learning algorithms with better context sets.

Muller *et al.* [43] and Al-Shedivat *et al.* [3] compare traditional active learning algorithms for few-shot text and image classification at training time, i.e. active $\text{Pick}_\theta^{\text{train}}$, passive $\text{Pick}_\theta^{\text{eval}}$. Boney *et al.* [9] instead compare active learning algorithms inside $\text{Pick}_\theta^{\text{eval}}$, specifically when f_θ is a ProtoNet, with passive $\text{Pick}_\theta^{\text{train}}$. (They do this in semi-supervised few-shot image classification; more discussion on the relationship of active meta-learning to active semi-supervised few-shot learning is provided in Appendix C.) Active $\text{Pick}_\theta^{\text{train}}$ and $\text{Pick}_\theta^{\text{eval}}$ are both feasible settings, but as argued above, if we are concerned with performance of our deployed predictor we should use an active $\text{Pick}_\theta^{\text{eval}} = \text{Pick}_\theta^{\text{deploy}}$. One can choose $\text{Pick}_\theta^{\text{train}}$ to be active or not, depending on which learns better predictors; we show in Appendix N that active $\text{Pick}_\theta^{\text{train}}$ does not seem to help.

Stratification In passive few-shot classification, the Pick functions typically choose context points according to a *stratified* sample: for one-shot classification, \mathcal{C} contains exactly one point per class. This is because, if we take a uniform random sample of size N for an N -way classification problem, \mathcal{C} is unlikely to

contain all the classes, making classification very difficult. Assuming “nature” gives a stratified uniform sample, as in nearly all work on few-shot classification, also seems reasonable.

In pool-based active settings, however, it is highly unreasonable to assume that $\text{Pick}_\theta^{\text{deploy}}$ can be stratified (as illustrated on the left side of Fig. 1): to do so, we would need to know the label of every point in $\check{\mathcal{D}}$, in which case we should simply use all those labels. As we would like $\text{Pick}_\theta^{\text{eval}} = \text{Pick}_\theta^{\text{deploy}}$, eval-time stratification is then not particularly reasonable; even so, we do report such results per the standards of meta-learning. When $\text{Pick}_\theta^{\text{deploy}}$ is unstratified (as in the right side of Fig. 1), it is particularly important for the selection criterion to find samples from each class.

Train-time stratification with unstratified evaluation does not leak data labels, and is plausible when $\mathcal{P}^{\text{train}}$ and $\mathcal{P}^{\text{eval}}$ are fully labeled. Since this approach trains f_θ in an “easy” setting and evaluates it in a “hard” one, however, we will see it tends to slightly underperform the fully-unstratified default. Regression tasks are not typically stratified; we do not stratify for regression experiments.

2.2 Related Work: Meta-Learning algorithms

Meta-learning algorithms can be divided into several categories; all will be applicable for our active learning strategies, and we evaluate with at least one representative algorithm per category.

Metric-based methods learn a representation space encoding a “good” similarity, where simple classifiers work well [49, 64]. ProtoNet [61] finds features so that points from each class are close to the prototype feature of the class.

Optimization-based methods use f_θ that incorporate optimization, e.g. gradient descent as in MAML [4, 17], which seeks parameters θ such that gradient descent quickly finds a useful model on a new task. ANIL [51] freezes most of the network and only updates the last layer, while R2D2 [7] and MetaOptNet [40] replace the last layer with a convex problem whose solution can be differentiated; these approaches can improve both performance and speed.

Model-based methods learn a model that explicitly adapts to new tasks, typically by modeling the distribution of y from \mathcal{T} given its x values and \mathcal{C} . The most prominent family of methods is Neural Processes (NPs) [15, 21], which encode a context set and estimate task-specific distribution parameters. Conditional NPs can have issues with underfitting [20, 21], but AttentiveNPs [35] and ConvNPs [25] are more robust. They are more commonly used for regression.

Pre-training methods, such as SimpleShot [68] and Baseline++ [12], are based on repeated demonstrations [24, 71] that simply pre-training a multi-class model can surpass the performance of commonly used meta-learners.

3 Active Learning

In pool-based active learning, a model requests labels for the most “informative” data points from a pool of unlabeled data. The key question is how to estimate which data points will be informative.

3.1 Related Work: Existing Active Learning Methods

Uncertainty-based methods Simple but effective uncertainty-based methods such as maximum entropy [67], least confident [59], and margin sampling [56] are widely used for active learning. Since they only consider current models’ uncertainty, active learning strategies that consider expected changes in model parameters [6, 60] and model outputs [18, 26, 33, 34, 42, 55, 63, 73] have been also been proposed. However, recent analyses have empirically demonstrated that at least in certain experimental settings, most active learning methods are not significantly different from one another [38], and may not even improve over random selection [44]. We consider the following methods from this category:

Random Uniformly randomly samples a context set from unlabeled set \mathcal{U} .

Entropy Add a point to the context set based on $x^* = \arg \max_{x \in \mathcal{U}} H(\hat{y}(x) | x)$, where $H(\cdot)$ is Shannon entropy [67]. Other than in Appendix K, we apply this in “batch mode,” i.e. we do not observe points one-by-one but rather choose the $|\mathcal{C}|$ points with the highest “initial” entropy.⁵

Margin Add a point to \mathcal{C} based on $x^* = \arg \min_{x \in \mathcal{U}} p_1(y|x) - p_2(y|x)$, where p_1 and p_2 denote the first and second highest predicted probabilities, respectively [56]. We also run this method in “batch mode.”

Although Entropy and Margin are very simple and fast to evaluate, no uncertainty-based method seems to substantially outperform them on typical active image classification tasks (see *e.g.* [42]), and we will see that other methods are unlikely to be competitive in low-budget regimes.

Low-budget active learning The limitations of typical active learning approaches may especially apply in very-low-budget cases, such as those considered in few-shot classification and meta-learning. In particular, when the “current” model is quite bad, using it to choose points might be counterproductive. In the one-shot case especially, standard active learning methods simply do not apply.

Recently, several papers have have proposed novel active learning algorithms for these settings; none of these papers focused on meta-learning, but should be broadly applicable since meta-learning is also a low-budget setting. Rather than picking *e.g.* the points about which a model is least certain, these papers propose to label the “most representative” data points independently of a “current” model.

DPP Determinantal Point Processes (DPPs) query diverse samples, by selecting a subset that maximizes the determinant of a similarity matrix [8].

⁵ Traditional active learning methods would generally retrain between each step, requiring a back-and-forth labeling process not needed by the methods discussed shortly. In modern deep learning settings, this is almost never done due to the expense of retraining; “batch-mode” entropy is still excellent in those settings [38, 42]. Appendix K explores more frequent retraining; the takeaway results are overall similar to the rest of our experiments.

- Typiclust** Run k -means on the unlabeled data points, where $k = |\mathcal{C}|$ is the annotation budget. Select one data point per cluster such that the distance between a data point and its k' nearest neighbors is minimized: $\arg \min_{x \in \mathcal{U}} \sum_{x' \in \text{NN}_{k'}(x)} \|x - x'\|_2$ [27].
- Coreset** Select a subset of the unlabeled set \mathcal{U} to approximately minimize the distance from unlabeled data points to their nearest labeled point [57].
- ProbCover** Select data points that roughly maximize the number of unlabeled points within a distance of δ from any labeled point, where δ is chosen according to a “purity” heuristic [70]; see Appendix G for more details.

3.2 Features for Representative-Selection Methods

Notions of the “most representative” data points are highly dependent on a reasonable metric of data similarity. Prior methods operated either on raw data – typically a poor choice for complex datasets like natural images – or, in semi-supervised settings as in ProbCover and Typiclust, on SimCLR [11] features learned on the unlabeled data.

In metric-based meta-learning, we propose to instead use the current meta-learned representation; choosing points representative for the features we will use downstream is the natural choice. In MAML, the most natural equivalent might be features from the empirical neural tangent kernel (NTK) [39] of the current initialization network; this approximates what will happen when the network is trained on \mathcal{C} ,⁶ and so is perhaps the best simple understanding of “how this network views the data.” Even empirical NTKs are often expensive to evaluate, however, and we thus propose to instead use features from the penultimate layer of the initialization neural net $f_\theta(\{\})$, corresponding to the NTK of a model that only retrains its last layer (as in ANIL, R2D2, and MetaOptNet). We also use the penultimate-layer representations of $f_\theta(\{\})$ for NP-based meta-learning.

Experiments in Appendix J show that this proposal outperforms off-the-shelf self-supervised features like SimCLR.

3.3 Gaussian Mixture Selection for Low-Budget Active Learning

We propose the following very simple algorithm for low-budget active learning: fit a mixture of k Gaussians to the unlabeled data features, where k is the label budget, using EM with a k -means initialization. We use a shared diagonal covariance matrix (more details about EM are provided in Appendix L). Once a mixture is fit, we select the highest-density point from each component:

$$x^* = \arg \min_{x \in \mathcal{U}} (x - \mu_j)^\top \Sigma^{-1} (x - \mu_j) \text{ for each } j \in [k]. \quad (4)$$

⁶ Theoretical results about the NTK technically depend on a random initialization, which is not the case here. Mohamadi *et al.* [42] provide some assurance in that if the initialization were obtained by gradient descent on some dataset, the results would still hold, but MAML finds initial parameters differently.

Algorithm 1: GMM-based Active Meta-learning

Input: Selection distribution $\text{Pick}_{\theta}^{\{\text{train}, \text{eval}\}}$, a learning algorithm f_{θ} , empirical risk \mathcal{R}_{ℓ} , and the size of context sets k

- 1 Find $\hat{\theta}$ using Eq. (1) where $\text{Pick}_{\theta}^{\text{train}}$ may be stratified // **Meta-train**
- 2 **while** task for evaluation exists **do** // **Meta-test**
- 3 $\tilde{\mathcal{D}} \sim P^{\text{eval}}$ and sample $\tilde{\mathcal{T}}$ from $\tilde{\mathcal{D}}$
- 4 Fit GMM: $\{(\hat{\pi}_j, \hat{\mu}_j, \hat{\Sigma}_j)\}_{j=1}^k$ using Eq. (10)–(12) in Appendix L
- 5 Select $\{x_j^*\}_{j=1}^k$ such that $\forall j \in [k], x_j^* = \arg \min_{x \in \mathcal{X}} (x - \hat{\mu}_j)^T \hat{\Sigma}_j (x - \hat{\mu}_j)$
- 6 Annotate $\{x_j^*\}_{j=1}^k$ to create $\tilde{\mathcal{C}}$, and evaluate $f_{\hat{\theta}}$ using $R_{\ell}(f_{\hat{\theta}(\tilde{\mathcal{C}})}, \tilde{\mathcal{T}})$

The proposed method is summarized in Algorithm 1.

For metric-based meta-learning, the motivation of this algorithm is clear: we want labeled points that approximately “cover” the data points. Our notion of a “cover” is somewhat different from that of Coreset [57] or ProbCover [70]; we avoid ProbCover’s need for a fixed radius, which we show can lead to poor choices (see Appendix G), and are more concerned with “average” covering (and hence perhaps less sensitive to outliers) than Coreset. The quality of selected data points from those methods are compared for a few metrics in Fig. 5.

On ANIL and MetaOptNet: since $|\mathcal{C}|$ is at most, say, 50 (in 10-way 5-shot) and the feature dimension is typically at least 100, ANIL becomes approximately the same multi-class max-margin separator obtained by (unregularized) MetaOptNet.⁷ Intuitively, as $|\mathcal{C}|$ grows, the means of an isotropic Gaussian mixture converge to roughly a covering set for the dataset \mathcal{U} , and the max-margin separator of a set cover for \mathcal{U} will be similar to the max-margin separator for all of the data. Even in various cases when $|\mathcal{C}| \ll |\mathcal{U}|$, choosing the means yields a max-margin separator that generalizes well.

Figure 2 illustrates that, if class-conditional data distributions are isotropic Gaussians with the same covariance matrices, labeling the cluster centers can be far preferable to labeling a random point from each cluster. This is backed up by the following theoretical results, which are all proved in Appendix A.

Proposition 1. *Suppose that $\{x_i\}_{i=1}^N$ are orthonormal. Then, the solution to (6) with the dataset $\{(x_y, y)\}_{y=1}^N$ is given by $w_y = x_y - \frac{1}{N} \sum_{i=1}^N x_i$, and hence*

$$\text{for any } x, \quad \arg \max_y w_y^{\top} x = \arg \min_y \|x - x_y\|. \quad (5)$$

Proposition 1 says with orthonormal data points, a N -class support vector machine (one form of max-margin separators) defined in Eq. (6) becomes a nearest-neighbor classifier. While these assumptions will not exactly hold in practice, for high-dimensional normalized features, it is reasonable to expect our selected data points to be *almost* orthonormal. In combination with Lemma 1 (in Appendix A), this leads to the following optimality result.

⁷ For reasonable distributions and networks, \mathcal{C} is almost surely linear separable; thus ANIL, which is gradient descent for logistic regression, will converge to the multi-class max-margin separator [62].

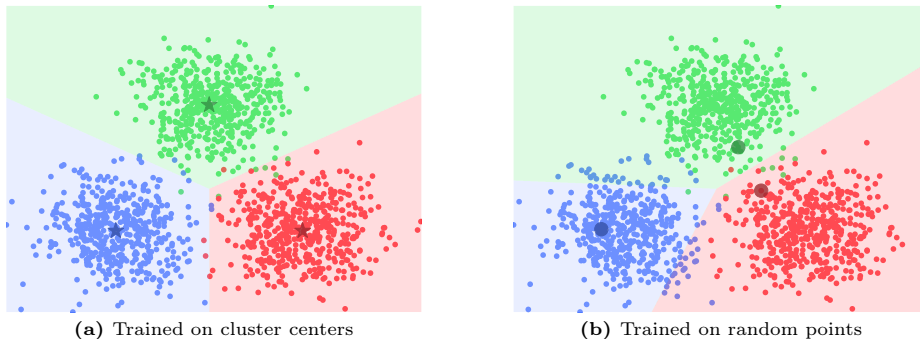


Fig. 2: Decision boundaries using a multi-class SVM (6) trained on a one-shot dataset containing (a) cluster centers (stars) and (b) randomly selected points (circles).

Corollary 1. *Suppose $Y \sim \text{Uniform}([N])$, and $X \mid (Y = y) \sim \mathcal{N}(\mu_y, \sigma^2 I)$, where the μ_i are orthonormal. Then the max-margin separator (6) on $\{(\mu_i, i)\}_{i=1}^N$ is Bayes-optimal for $Y \mid (X = x)$.*

For more general settings, we argue that GMM is still a good method based on being an efficient set cover, as shown in Fig. 4 in Appendix A.

Very-low-budget regime Active learning based on Gaussian mixtures is not new in and of itself. Closely-related methods such as k -means, k -means⁺⁺ or k -medoids have been employed either as standalone selection algorithms [2, 65] or in combination with uncertainty-based methods [6, 14, 27, 45]. Some recent work [9] including DPP [8] and Coreset [57] show significant improvements over k -means baselines. These trends, however, do not seem to hold true in the very-low-budget scenarios typically encountered in meta-learning. As shown in Fig. 8, GMM matches or outperforms other low-budget methods with very small numbers of labels for standard image classification tasks, which has not been known in the community. The following section shows that GMM provides substantial improvements in meta-learning.

4 Active Meta-Learning Experiments

We now compare various active learning methods for variants of active meta learning as defined in Sec. 2.1, both for classification tasks (in Secs. 4.1 to 4.3) and regression (in Sec. 4.4).

4.1 Few-shot Image Classification

We use four popular few-shot image classification benchmark datasets. **MiniImageNet** [52, 64] consists of 60 000 images with 64 training classes, 16 validation, and 20 test. **TieredImageNet** [53] consists of 20 training super-classes, 6 validation, and 8 test; each contains 10 to 30 sub-classes. **FC100** [49] consists of 60

training classes, 20 validation, and 20 test. **CUB** [29,66] consists of 200 classes of bird images, with 140 training classes, 30 validation, and 30 test.

We validate if our active learning method works across various types of meta-learning methods. We run⁸ metric-based: ProtoNet [61], optimization-based: MAML [17], ANIL [51], and MetaOpt [40], as well as pre-training-based: Baseline++ [12] and SimpleShot [68].⁹ We vary the backbone to demonstrate robustness: for instance, we use 4 convolutional blocks for MAML and ProtoNet, and ResNet10 [28] for Baseline++. As typical in few-shot classification, we report means and 95% confidence intervals for test accuracy on 600 meta-test samples.

We use the meta-learner’s features as proposed in Sec. 3.2 for all methods; experiments in Appendix J confirm that they outperform contrastive learning of features on the meta-training set. Additionally, in the main body we only present results where $\text{Pick}_\theta^{\text{train}}$ is random; Appendix N demonstrates that, in our setup, active learning at train time is actually mildly *harmful* to overall performance, aligning with observations by Ni *et al.* [46] and Setlur *et al.* [58].

For **metric-based** methods, Tab. 1 shows results for ProtoNet on FC100. The simple GMM method significantly outperforms the other active learning methods on all problems considered here. As reported [27,70], uncertainty-based methods are significantly worse than random selection in this low-budget regime.

For **optimization-based**, Tab. 2 shows results with MAML on MiniImageNet. GMM again outperforms the other methods in most cases. The performance of ProbCover is sometimes much lower than other methods due to its radius parameter, which is very difficult to tune, with the best choice changing dramatically depending on the sub-task although [70] propose to fix this parameter per dataset (see Appendix G for more). Additional results for ANIL on TieredImageNet and MetaOptNet on FC100 are provided in Appendix H.

For **pre-training-based** methods, we compare active learning strategies with Baseline++ on the CUB dataset in Tab. 3, seeing that the proposed method is again usually by far the best, though in one five-shot case it essentially ties with DPP. As these methods do not follow the meta-training process in (1), train-time stratification is not applicable. Appendix H shows results for SimpleShot.

Comparison between active learning methods. Fig. 3 (left) visualizes context set selection using t-SNE [41] for one 5-way, 1-shot, unstratified task. It is vital to select one sample from each class; only GMM does so here. Figure 3 (right) summarizes behavior across many tasks; while not perfect, GMM does a much better job of selecting distinct classes.

Entropy and **Margin** are typically far worse than random. So is **Coreset**, agreeing with prior observations [6,27,70]; this may be because of issues with the greedy algorithm and/or sensitivity to outliers. **Typiclust** tends to pick points which, while dense according to its “typicality measure,” are far from cluster

⁸ We reproduce ProtoNet, MAML, and ANIL using Learn2Learn [5]; for MetaOptNet, Baseline++, and SimpleShot, we use repositories provided by the authors.

⁹ We do not run a model-based method on this case, though we will in Sec. 4.4; most variants do not work well conditioning on images.

Pick $_{\theta}^{eval}$	1-Shot			5-Shot		
	Fully strat.	Train strat.	Unstrat.	Fully strat.	Train strat.	Unstrat.
Random	36.73 \pm 0.18	31.27 \pm 0.21	31.40 \pm 0.41	47.98 \pm 0.18	42.83 \pm 0.20	44.00 \pm 0.21
Entropy	33.67 \pm 0.16	29.82 \pm 0.20	30.01 \pm 0.20	44.64 \pm 0.17	38.39 \pm 0.22	38.36 \pm 0.25
Margin	34.28 \pm 0.18	29.74 \pm 0.20	28.99 \pm 0.20	45.31 \pm 0.17	39.65 \pm 0.21	38.13 \pm 0.24
DPP	36.20 \pm 0.18	31.34 \pm 0.20	31.09 \pm 0.20	47.53 \pm 0.17	43.69 \pm 0.20	44.19 \pm 0.20
Coreset	35.79 \pm 0.17	30.31 \pm 0.20	31.57 \pm 0.18	43.08 \pm 0.40	41.56 \pm 0.20	41.79 \pm 0.22
Typiclust	46.01 \pm 0.16	30.96 \pm 0.19	30.61 \pm 0.21	47.54 \pm 0.17	43.61 \pm 0.18	44.03 \pm 0.21
ProbCover	48.66 \pm 0.16	32.86 \pm 0.22	33.58 \pm 0.19	51.11 \pm 0.17	44.20 \pm 0.23	44.40 \pm 0.24
GMM (Ours)	50.22 \pm 0.18	34.23 \pm 0.23	35.03 \pm 0.23	54.76 \pm 0.17	46.30 \pm 0.21	47.03 \pm 0.20

Table 1: 5-Way K-Shot on FC100 with ProtoNet, with Pick $_{\theta}^{train}$ random. The **first**, **second**, **third** best results for each setting are marked in this and all other tables.

Pick $_{\theta}^{eval}$	1-Shot			5-Shot		
	Fully strat.	Train strat.	Unstrat.	Fully strat.	Train strat.	Unstrat.
Random	47.93 \pm 0.20	28.16 \pm 0.17	34.85 \pm 0.19	64.16 \pm 0.18	53.54 \pm 0.20	58.84 \pm 0.20
Entropy	48.16 \pm 0.20	25.56 \pm 0.14	30.44 \pm 0.17	61.22 \pm 0.20	34.36 \pm 0.23	39.57 \pm 0.26
Margin	48.31 \pm 0.20	28.32 \pm 0.16	30.83 \pm 0.17	63.73 \pm 0.18	49.24 \pm 0.22	53.92 \pm 0.22
DPP	48.96 \pm 0.21	28.90 \pm 0.17	36.44 \pm 0.19	64.15 \pm 0.18	54.18 \pm 0.20	57.86 \pm 0.19
Coreset	47.74 \pm 0.20	29.19 \pm 0.18	33.71 \pm 0.18	61.28 \pm 0.18	30.98 \pm 0.19	45.74 \pm 0.23
Typiclust	55.65 \pm 0.18	27.45 \pm 0.17	35.46 \pm 0.18	64.16 \pm 0.18	46.70 \pm 0.21	57.83 \pm 0.21
ProbCover	52.07 \pm 0.17	23.34 \pm 0.11	37.29 \pm 0.18	64.66 \pm 0.18	40.01 \pm 0.21	45.32 \pm 0.22
GMM (Ours)	58.82 \pm 0.24	33.34 \pm 0.24	37.68 \pm 0.19	67.18 \pm 0.18	54.35 \pm 0.20	59.05 \pm 0.20

Table 2: 5-Way K-Shot on MiniImageNet with MAML, with Pick $_{\theta}^{train}$ random.

centers; this may be helpful in traditional active learning, but seems to hurt here. **DPP** is often better than random, but only barely.

ProbCover manages to cover the feature space well, and is usually second-best. However, its “hard” radius causes issues; it may be preferable to use a smoother notion, as in GMM. The “purity” heuristic to choose δ also does not seem to align well with performance for meta-learning, as shown in Appendix G. Appendix M further analyzes the poor performance of other methods.

GMM provides robust performance with few new hyperparameters.¹⁰

“Soft” k -means would be a special case of GMM with a spherical covariance. For some cases, standard k -means performs about the same as GMM, but GMM is occasionally much better: for Baseline++ on CUB, GMM outperforms k -means by 3.95 points for 5-way 1-shot and 11.79 for 5-shot. We provide a more thorough comparison to k -means in Appendix F.

4.2 Comparison with Hybrid Active Learning Methods

We compare the proposed GMM method with “hybrid” methods that select data points for annotation using both uncertainty and representation measures.¹¹

¹⁰ We did not significantly tune k -means or EM parameters from standard defaults.

¹¹ We separate the comparison with hybrid to highlight it, because hybrid methods are often considered better than solely uncertainty- or representation-based methods.

$\text{Pick}_\theta^{eval}$	1-Shot		5-Shot	
	Test strat.	Test unstrat.	Test strat.	Test unstrat.
Random	68.44 ± 0.92	51.03 ± 0.88	82.66 ± 0.56	79.57 ± 0.67
Entropy	66.33 ± 0.91	45.31 ± 0.89	80.97 ± 0.60	78.33 ± 0.72
Margin	68.65 ± 0.90	50.48 ± 0.94	82.29 ± 0.64	71.07 ± 0.83
DPP	71.53 ± 0.89	54.38 ± 0.92	82.81 ± 0.55	78.62 ± 0.76
Coreset	69.01 ± 0.91	56.22 ± 0.94	82.07 ± 0.55	76.35 ± 0.74
Typiclust	70.58 ± 0.81	29.80 ± 0.32	74.86 ± 0.81	70.00 ± 0.92
ProbCover	78.11 ± 0.69	55.09 ± 0.98	78.59 ± 0.64	65.71 ± 0.97
GMM (Ours)	79.98 ± 0.60	59.55 ± 0.87	82.55 ± 0.58	82.68 ± 0.57

Table 3: 5-Way K-Shot on CUB with Baseline++, with $\text{Pick}_\theta^{train}$ random.

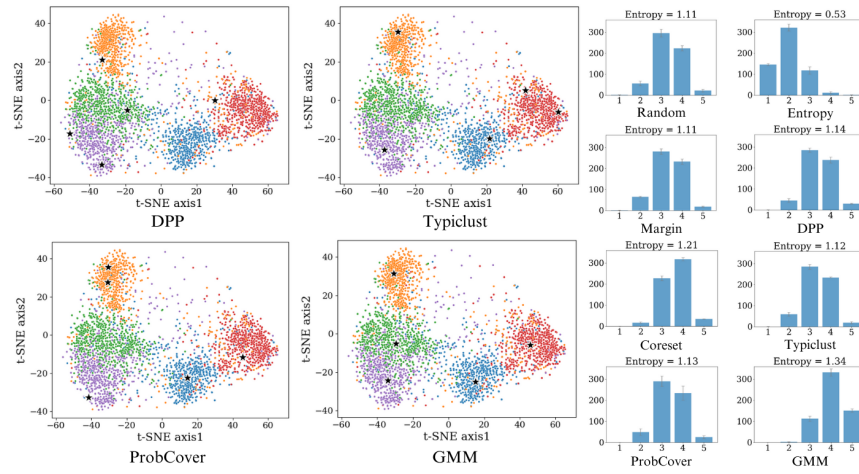


Fig. 3: **Left.** t-SNE of unlabeled points of one 5-way, 1-shot, unstratified MiniImageNet task. Stars denote selected context points using each method. **Right.** Distributions of the number of classes selected in each $\tilde{\mathcal{C}}$ by ProtoNet on MiniImageNet among 600 meta-test cases, along with the mean empirical entropy of y from $\tilde{\mathcal{C}}$. The higher the value is, the more diverse classes are selected; $\log 5 \approx 1.6$ would be perfect.

Weighted Entropy Nguyen *et al.* [45] propose weighted expected error for binary classification. For multi-class cases, we derive that it becomes weighted entropy, where weights are likelihood computed using soft k -means.

BADGE This method [6] selects points using k -means⁺⁺ with embeddings derived from the gradients of loss w.r.t the weights of the last layer.

k -means Entropy This approach [3] first clusters unlabeled samples using k -means⁺⁺, then selects samples per cluster using the classifier’s entropy.

Tab. 4 shows that the proposed GMM-based method significantly outperforms all the hybrid methods. This experiment, along with the poor performance of

Data & Model	Clustering	1-Shot		5-Shot	
		Train strat.	Unstrat.	Train strat.	Unstrat.
MiniImage. MAML	Weighted Ent.	22.69 \pm 0.18	32.27 \pm 0.32	23.75 \pm 0.25	46.80 \pm 0.33
	BADGE	27.71 \pm 0.18	34.30 \pm 0.21	41.37 \pm 0.28	58.79 \pm 0.24
	k -means Ent.	30.59 \pm 0.28	33.73 \pm 0.24	38.24 \pm 0.29	54.87 \pm 0.26
	GMM (Ours)	33.34 \pm 0.24	37.68 \pm 0.19	54.35 \pm 0.20	59.05 \pm 0.20
FC100 ProtoNet	Weighted Ent.	31.80 \pm 0.20	28.94 \pm 0.19	40.40 \pm 0.25	39.95 \pm 0.25
	BADGE	30.91 \pm 0.23	29.29 \pm 0.28	43.85 \pm 0.22	44.00 \pm 0.29
	k -means Ent.	30.93 \pm 0.22	30.43 \pm 0.24	41.76 \pm 0.27	43.41 \pm 0.29
	GMM (Ours)	34.23 \pm 0.23	35.03 \pm 0.23	46.30 \pm 0.21	47.03 \pm 0.20

Table 4: Comparison of GMM with hybrid active learning methods.

$\text{Pick}_{\theta}^{eval}$	P^{eval} on Places		P^{eval} on CUB	
	1-Shot	5-Shot	1-Shot	5-Shot
Random	44.28 \pm 1.93	77.92 \pm 1.70	49.93 \pm 0.92	84.38 \pm 0.72
Entropy	36.12 \pm 1.25	57.79 \pm 2.93	41.85 \pm 0.99	71.15 \pm 0.99
Margin	43.31 \pm 1.97	73.65 \pm 1.94	48.04 \pm 0.98	78.84 \pm 0.92
DPP	46.76 \pm 2.29	78.36 \pm 1.89	51.41 \pm 0.90	84.19 \pm 0.72
Coreset	50.03 \pm 0.93	65.20 \pm 2.77	50.77 \pm 0.95	81.80 \pm 0.81
Typiclust	43.76 \pm 1.98	77.57 \pm 1.84	43.39 \pm 1.03	50.69 \pm 1.08
ProbCover	47.93 \pm 1.08	59.08 \pm 2.50	62.13 \pm 1.08	69.80 \pm 1.16
GMM (Ours)	60.01 \pm 0.86	86.45 \pm 1.42	59.87 \pm 0.86	85.49 \pm 0.67

Table 5: Cross-domain meta-learning tasks using a ResNet18 pre-trained on ImageNet.

uncertainty methods such as Entropy, demonstrates that for the very-low-budget regime, diversity is significantly more important than reducing uncertainty.

4.3 Cross-Domain Active Meta-Learning

Cross-domain learning, where \mathcal{P}^{train} is “fundamentally different” from \mathcal{P}^{eval} , is typically more difficult than “in-domain” meta-learning. We use a ResNet18 [28] pretrained with standard supervised learning on ImageNet, and meta-test on CUB and **Places** [72], which contains images of “places” such as restaurants. As used for cross-domain meta-learning by [48], it contains 16 classes with an average of 1,715 images each. As the model is not meta-trained, train stratification is not relevant; we show results in Tab. 5 only for unstratified test sets. GMM is again the clear overall winner; other methods are often worse than random.

Discussion Most uncertainty measures tend to be high near decision boundaries. This may be sub-optimal in low-budget settings, as these uncertain points often represent outliers, or are too challenging to generalize.

Active Strategy	Sine (3-Shots)	Distractor (2-Shots)		ShapeNet1D (2-Shots)	
		IC	CC	IC	CC
Random	24.17 ± 0.43	18.91 ± 2.13	25.79 ± 2.17	16.52 ± 1.08	19.07 ± 1.30
DPP	23.19 ± 0.51	18.08 ± 2.12	19.68 ± 1.92	11.83 ± 0.85	13.68 ± 0.93
Coreset	31.36 ± 0.48	19.58 ± 1.95	24.08 ± 2.19	11.39 ± 0.91	13.05 ± 1.18
Typiclust	21.59 ± 0.40	20.27 ± 2.15	24.96 ± 2.68	12.54 ± 1.08	14.58 ± 1.24
ProbCover	29.36 ± 0.49	21.96 ± 2.45	25.25 ± 2.78	12.31 ± 0.85	13.95 ± 1.08
GMM (Ours)	18.09 ± 0.38	17.95 ± 2.05	22.03 ± 2.42	10.78 ± 0.72	12.35 ± 0.97

Table 6: Meta-learning for regression on a toy dataset and two pose estimation datasets for Intra-Category (IC) and Cross-Category (CC). Sine func. and Distractor use mean squared error, ShapeNet1D uses cosine-sine-distance; lower values are better for each.

The primary purpose of context sets in meta-learning is to inform predictions on target samples, necessitating the selection of easily referable points. If the selected context samples are too distant from the target samples, making accurate predictions for the target set becomes difficult. Diversity measures, particularly GMM, ensure that the context set remains close to the target set even in adverse scenarios, such as when target samples are outliers (see Fig. 2). Thus, it is preferable to solely consider diversity for active selection of context sets.

While hybrid methods that incorporate both uncertainty and diversity may be beneficial in mid or high-budget active learning scenarios, they provide limited assistance in extremely low-budget scenarios such as meta-learning.

4.4 Active Meta-Learning for Regression

Each **sinusoidal function** [17] has task $y = a \sin(x + p)$, where $a \sim \text{Unif}(0.1, 5)$ is the amplitude, and $p \sim \text{Unif}(0, \pi)$ is the phase of sine functions; we use MAML for this dataset. **Distractor** and **ShapeNet1D** are vision regression datasets [19]; the task is to predict the position of a specific object in an image ignoring a distractor, or to predict an object’s 1D pose (azimuth rotation). **IC** uses objects whose classes were observed during meta-training, while **CC** has novel object classes. We use conditional Neural Processes (NP) for Distractor, and attentive NP for ShapeNet1D. Details are provided in Appendix I.

Table 6 compares active strategies on these datasets; GMM again performs generally the best, followed by Coreset and DPP instead of ProbCover.

5 Conclusion

We clarified the ways in which active learning can be incorporated into meta-learning. While active context set selection does not seem to work at meta-train time (Appendix N), it can be extremely useful at meta-testing/deployment time.

We proposed a surprisingly simple method that substantially outperforms previous proposals. It is intuitive, very easy to implement, and bears theoretical guarantees in a particular “stylized” but informative situation.

Acknowledgements

This work was enabled in part by support provided by the Natural Sciences and Engineering Research Council of Canada, the Canada CIFAR AI Chairs program, Mitacs through the Mitacs Accelerate program, Calcul Québec, the BC DRI Group, and the Digital Research Alliance of Canada.

References

1. Agarwal, M., Yurochkin, M., Sun, Y.: On sensitivity of meta-learning to support data. In: NeurIPS (2021)
2. Aghaei, A., Ghadiri, M., Baghshah, M.S.: Active distance-based clustering using k-medoids. In: PAKDD (2016)
3. Al-Shedivat, M., Li, L., Xing, E., Talwalkar, A.: On data efficiency of meta-learning. In: AISTAT (2021)
4. Antoniou, A., Edwards, H., Storkey, A.: How to train your MAML. In: ICLR (2019)
5. Arnold, S.M.R., Mahajan, P., Datta, D., Bunner, I., Zarkias, K.S.: learn2learn: A library for Meta-Learning research (2020)
6. Ash, J.T., Zhang, C., Krishnamurthy, A., Langford, J., Agarwal, A.: Deep batch active learning by diverse, uncertain gradient lower bounds. ICLR (2020)
7. Bertinetto, L., Henriques, J.F., Torr, P.H.S., Vedaldi, A.: Meta-learning with differentiable closed-form solvers. In: ICLR (2019)
8. Bıyık, E., Wang, K., Anari, N., Sadigh, D.: Batch active learning using determinantal point processes. NeurIPS (2019)
9. Boney, R., Ilin, A.: Semi-supervised and active few-shot learning with prototypical networks. arXiv preprint arXiv:1711.10856 (2017)
10. Chang, A.X., Funkhouser, T., Guibas, L., Hanrahan, P., Huang, Q., Li, Z., Savarese, S., Savva, M., Song, S., Su, H., Xiao, J., Yi, L., Yu, F.: ShapeNet: An information-rich 3D model repository. arXiv preprint arXiv:1512.03012 (2015)
11. Chen, T., Kornblith, S., Norouzi, M., Hinton, G.: A simple framework for contrastive learning of visual representations. In: ICML (2020)
12. Chen, W.Y., Liu, Y.C., Kira, Z., Wang, Y.C.F., Huang, J.B.: A closer look at few-shot classification. In: ICLR (2019)
13. Crammer, K., Singer, Y.: On the algorithmic implementation of multiclass kernel-based vector machines. JMLR (2001)
14. Donmez, P., Carbonell, J.G., Bennett, P.N.: Dual strategy active learning. In: ECML (2007)
15. Dubois, Y., Gordon, J., Foong, A.Y.: Neural process family. <http://yanndubs.github.io/Neural-Process-Family/> (2020)
16. Fang, M., Li, Y., Cohn, T.: Learning how to active learn: A deep reinforcement learning approach. In: EMNLP (2017)
17. Finn, C., Abbeel, P., Levine, S.: Model-agnostic meta-learning for fast adaptation of deep networks. In: ICML (2017)
18. Freytag, A., Rodner, E., Denzler, J.: Selecting influential examples: Active learning with expected model output changes. In: ECCV (2014)
19. Gao, N., Ziesche, H., Vien, N.A., Volpp, M., Neumann, G.: What matters for meta-learning vision regression tasks? In: CVPR (2022)
20. Garnelo, M., Rosenbaum, D., Maddison, C., Ramalho, T., Saxton, D., Shanahan, M., Teh, Y.W., Rezende, D., Eslami, S.A.: Conditional neural processes. In: ICML (2018)

21. Garnelo, M., Schwarz, J., Rosenbaum, D., Viola, F., Rezende, D.J., Eslami, S., Teh, Y.W.: Neural processes. In: ICML Workshop on Theoretical Foundations and Applications of Deep Generative Models (2018)
22. Garnett, R., Krishnamurthy, Y., Xiong, X., Schneider, J., Mann, R.: Bayesian optimal active search and surveying. In: ICML (2012)
23. Gautier, G., Polito, G., Bardenet, R., Valko, M.: DPPy: DPP sampling with Python. JMLR-MLOSS (2019), <https://github.com/guilgautier/DPPy/>
24. Goldblum, M., Reich, S., Fowl, L., Ni, R., Cherepanova, V., Goldstein, T.: Unraveling meta-learning: Understanding feature representations for few-shot tasks. In: ICML (2020)
25. Gordon, J., Bruinsma, W.P., Foong, A.Y., Requeima, J., Dubois, Y., Turner, R.E.: Convolutional conditional neural processes. In: ICLR (2020)
26. Guo, Y., Greiner, R.: Optimistic active-learning using mutual information. In: IJCAI (2007)
27. Hachohen, G., Dekel, A., Weinshall, D.: Active learning on a budget: Opposite strategies suit high and low budgets. ICML (2022)
28. He, K., Zhang, X., Ren, S., Sun, J.: Deep residual learning for image recognition. In: CVPR (2016)
29. Hilliard, N., Phillips, L., Howland, S., Yankov, A., Corley, C.D., Hodas, N.O.: Few-shot learning with metric-agnostic conditional embeddings. arXiv preprint arXiv:1802.04376 (2018)
30. Hospedales, T., Antoniou, A., Micaelli, P., Storkey, A.: Meta-learning in neural networks: A survey. PAMI **44**(9), 5149–5169 (2022)
31. Huang, K., Geng, J., Jiang, W., Deng, X., Xu, Z.: Pseudo-loss confidence metric for semi-supervised few-shot learning. In: ICCV (2021)
32. Kaddour, J., Sæmundsson, S., Deisenroth, M.P.: Probabilistic active meta-learning. In: NeurIPS (2020)
33. Käding, C., Rodner, E., Freytag, A., Denzler, J.: Active and continuous exploration with deep neural networks and expected model output changes. In: NeurIPS Workshop on Continual Learning and Deep Networks (2016)
34. Käding, C., Rodner, E., Freytag, A., Mothes, O., Barz, B., Denzler, J., AG, C.Z.: Active learning for regression tasks with expected model output changes. In: BMVC (2018)
35. Kim, H., Mnih, A., Schwarz, J., Garnelo, M., Eslami, A., Rosenbaum, D., Vinyals, O., Teh, Y.W.: Attentive neural processes. In: ICLR (2019)
36. Konyushkova, K., Sznitman, R., Fua, P.: Learning active learning from data. In: NeurIPS (2017)
37. Kumar, R., Deleu, T., Bengio, Y.: The effect of diversity in meta-learning. In: AAAI (2022)
38. Lang, A., Mayer, C., Timofte, R.: Best practices in pool-based active learning for image classification (2021)
39. Lee, J., Xiao, L., Schoenholz, S., Bahri, Y., Novak, R., Sohl-Dickstein, J., Pennington, J.: Wide neural networks of any depth evolve as linear models under gradient descent. In: NeurIPS (2019)
40. Lee, K., Maji, S., Ravichandran, A., Soatto, S.: Meta-learning with differentiable convex optimization. In: CVPR (2019)
41. van der Maaten, L., Hinton, G.: Visualizing data using t-sne. JMLR (2008)
42. Mohamadi, M.A., Bae, W., Sutherland, D.J.: Making look-ahead active learning strategies feasible with neural tangent kernels. In: NeurIPS (2022)
43. Müller, T., Pérez-Torró, G., Basile, A., Franco-Salvador, M.: Active few-shot learning with fasl. In: NLDB (2022)

44. Munjal, P., Hayat, N., Hayat, M., Sourati, J., Khan, S.: Towards robust and reproducible active learning using neural networks. In: CVPR (2022)
45. Nguyen, H.T., Smeulders, A.: Active learning using pre-clustering. In: ICML (2004)
46. Ni, R., Goldblum, M., Sharaf, A., Kong, K., Goldstein, T.: Data augmentation for meta-learning. In: ICML (2021)
47. Nikoloska, I., Simeone, O.: Bamld: Bayesian active meta-learning by disagreement. SPAWC (2022)
48. Oh, J., Kim, S., Ho, N., Kim, J.H., Song, H., Yun, S.Y.: Understanding cross-domain few-shot learning based on domain similarity and few-shot difficulty. In: NeurIPS (2022)
49. Oreshkin, B., Rodríguez López, P., Lacoste, A.: Tadam: Task dependent adaptive metric for improved few-shot learning. In: NeurIPS (2018)
50. Pezeshkpour, P., Zhao, Z., Singh, S.: On the utility of active instance selection for few-shot learning. In: HAMLETS workshop at NeurIPS (2020)
51. Raghu, A., Raghu, M., Bengio, S., Vinyals, O.: Rapid learning or feature reuse? towards understanding the effectiveness of maml. In: ICLR (2020)
52. Ravi, S., Larochelle, H.: Optimization as a model for few-shot learning. In: ICLR (2017)
53. Ren, M., Triantafillou, E., Ravi, S., Snell, J., Swersky, K., Tenenbaum, J.B., Larochelle, H., Zemel, R.S.: Meta-learning for semi-supervised few-shot classification. In: ICLR (2018)
54. Ren, P., Xiao, Y., Chang, X., Huang, P.Y., Li, Z., Gupta, B.B., Chen, X., Wang, X.: A survey of deep active learning. ACM Comput. Surv. **54**(9) (10 2021)
55. Roy, N., McCallum, A.: Toward optimal active learning through monte carlo estimation of error reduction. In: ICML (2001)
56. Scheffer, T., Decomain, C., Wrobel, S.: Active hidden markov models for information extraction. In: ISIDA (2001)
57. Sener, O., Savarese, S.: Active learning for convolutional neural networks: A core-set approach. ICLR (2018)
58. Setlur, A., Li, O., Smith, V.: Is support set diversity necessary for meta-learning? NeurIPS Workshop (2020)
59. Settles, B.: Active learning literature survey (2009)
60. Settles, B., Craven, M., Ray, S.: Multiple-instance active learning. In: NeurIPS (2007)
61. Snell, J., Swersky, K., Zemel, R.S.: Prototypical networks for few-shot learning. In: NeurIPS (2017)
62. Soudry, D., Hoffer, E., Nacson, M.S., Gunasekar, S., Srebro, N.: The implicit bias of gradient descent on separable data. JMLR (2018)
63. Tan, W., Du, L., Buntine, W.: Diversity enhanced active learning with strictly proper scoring rules. In: NeurIPS (2021)
64. Vinyals, O., Blundell, C., Lillicrap, T., Wierstra, D., et al.: Matching networks for one shot learning. In: NeurIPS (2016)
65. Voevodski, K., Balcan, M.F., Röglin, H., Teng, S.H., Xia, Y.: Active clustering of biological sequences. JMLR (2012)
66. Wah, C., Branson, S., Welinder, P., Perona, P., Belongie, S.: The Caltech-UCSD Birds-200-2011 dataset. California Institute of Technology technical report CNS-TR-2011-001, California Institute of Technology (2011)
67. Wang, D., Shang, Y.: A new active labeling method for deep learning. In: IJCNN (2014)

- 68. Wang, Y., Chao, W.L., Weinberger, K.Q., van der Maaten, L.: Simpleshot: Revisiting nearest-neighbor classification for few-shot learning. arXiv preprint arXiv:1911.04623 (2019)
- 69. Wei, X.S., Xu, H.Y., Zhang, F., Peng, Y., Zhou, W.: An embarrassingly simple approach to semi-supervised few-shot learning. In: NeurIPS (2022)
- 70. Yehuda, O., Dekel, A., Hachohen, G., Weinshall, D.: Active learning through a covering lens. NeurIPS (2022)
- 71. Zhang, X., Meng, D., Gouk, H., Hospedales, T.M.: Shallow bayesian meta learning for real-world few-shot recognition. In: ICCV (2021)
- 72. Zhou, B., Lapedriza, A., Khosla, A., Oliva, A., Torralba, A.: Places: A 10 million image database for scene recognition. PAMI (2017)
- 73. Zhu, X., Lafferty, J., Ghahramani, Z.: Combining active learning and semi-supervised learning using gaussian fields and harmonic functions. In: ICML Workshops (2003)

A Details for Max-Margin Motivation

The following optimization problem is one form of an N -class max-margin problem, i.e. a multi-class support vector machine [13], on a training set $\{(x_i, y_i)\}_{i=1}^m$:

$$\min_{w_1, \dots, w_N} \sum_{y=1}^N \|w_y\|^2 \quad \text{s.t.} \quad \forall i \in [m], \forall y' \neq y_i, w_{y_i}^\top x_i \geq w_{y'}^\top x_i + 1. \quad (6)$$

This is a “hard” version of the problem used as a classification head by MetaOptNet [40], and can be obtained in their framework by taking the penalty parameter $C \rightarrow \infty$.

The decision boundaries obtained by small-step-size gradient descent for linear predictors with cross-entropy loss on separable data converge to those obtained by (6), as shown by Theorem 7 in Soudry *et al.* [62], for almost all datasets. Thus, ANIL [51], which uses gradient descent for linear predictors with cross-entropy loss on separable data, will approximately obtain the same solution when using enough steps with appropriately small learning rates.

MetaOptNet uses the homogeneous predictors discussed here. We can handle non-homogeneous linear predictors ($w^\top x + b$ instead of just $w^\top x$) with the standard trick of adding a constant 1 feature to each data point. This solution actually does not quite maximize the margin on the original problem, since it effectively adds b^2 to the objective in (6), but ANIL will find exactly this same solution when using gradient descent on a function with a separate intercept.

As visualized in Fig. 2 and explained in Sec. 3.3, if the class-conditional data distributions are isotropic Gaussians with the same covariance matrices, it is more advantageous to label the cluster centers than a random point from each cluster (supported by Corollary 1). We provide the proof for Corollary 1 below.

Corollary 1. *Suppose $Y \sim \text{Uniform}([N])$, and $X \mid (Y = y) \sim \mathcal{N}(\mu_y, \sigma^2 I)$, where the μ_i are orthonormal. Then the max-margin separator (6) on $\{(\mu_i, i)\}_{i=1}^N$ is Bayes-optimal for $Y \mid (X = x)$.*

Proof. Combine Proposition 1 and Lemma 1 below. \square

The orthonormal assumption keeps the proof tractable; far more analysis would be needed without it. With high-dimensional meta-learned features that are well-aligned to the learning problem, however, it is reasonable to expect that inner products between different classes will be much smaller than the within-class inner products.

This optimality result can break when the clusters do not share a spherical covariance; consider Fig. 4a, where the data is still Gaussian but the shared class-conditional covariance is not spherical. In the one-shot case, max-margin on the separators does not choose the optimal separator. In this case, we could manually select points to choose the correct line. Doing so, however, is quite risky; since we do not know the data labels (or that it is actually Gaussian), we might incorrectly separate the data. Figure 4b shows the same problem in a three-shot setting; here, even though the data is truly generated from a mixture

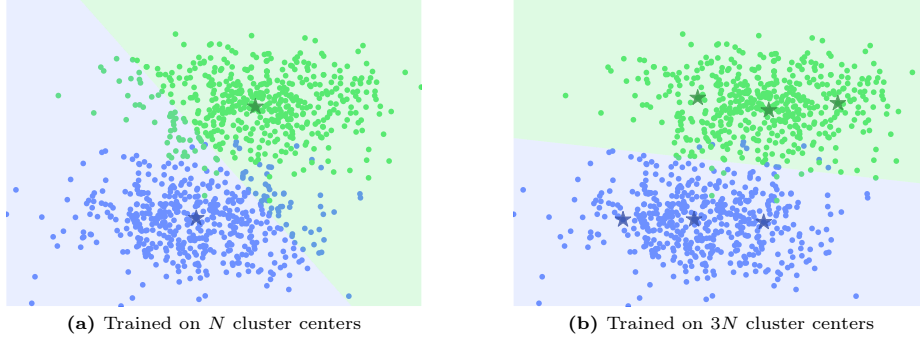


Fig. 4: Decision boundaries using a multiclass SVM (6) trained on cluster centers (shown by stars), with (a) the one-shot case and (b) the three-shot case.

of two Gaussians, fitting a mixture of six Gaussians gives us an approximate set cover of the data, and the max-margin separator now works well.

In fact, we can expect that (a) as the number of clusters grows, the cluster centers produce a better and better set cover of the dataset; (b) the max-margin separator on a set cover will approximate the max-margin separator on the full dataset, since the support vectors are all nearby.

A.1 Proofs

Proposition 1. *Suppose that $\{x_i\}_{i=1}^N$ are orthonormal. Then, the solution to (6) with the dataset $\{(x_y, y)\}_{y=1}^N$ is given by $w_y = x_y - \frac{1}{N} \sum_{i=1}^N x_i$, and hence*

$$\text{for any } x, \quad \arg \max_y w_y^\top x = \arg \min_y \|x - x_y\|. \quad (5)$$

Proof. We will be able to analytically solve the KKT conditions for (6) in this case. Rather than using existing analyses of (6), it will be simpler to directly analyze this particular case.

Let $\mathbf{w} = \begin{bmatrix} w_1 \\ \vdots \\ w_N \end{bmatrix} \in \mathbb{R}^{Nd}$, where d is the dimension of the x_i and w_y . The

objective of our optimization problem is then simply $\|\mathbf{w}\|^2$.

We will next define a matrix A such that the constraints can be written as $A\mathbf{w} + \mathbf{1} \leq \mathbf{0}$, with $A \in \mathbb{R}^{N(N-1) \times Nd}$ and \leq interpreted elementwise. Each constraint is of the form $-w_i^\top x_i + w_j^\top x_i + 1 \leq 0$, where $i \neq j$ are class indices in $[N]$. We can write the corresponding row of A as $(E_j - E_i)x_i$, where $E_i \in \mathbb{R}^{Nd \times d}$ are given by $E_i = \begin{bmatrix} 0_{(i-1)d \times d} \\ I_d \\ 0_{(N-i-1)d \times d} \end{bmatrix}$; these E_i are a block-matrix analogue

of standard basis vectors, so that $E_i x_i \in \mathbb{R}^{Nd}$ has x_i in the i th block of d coordinates, and 0 elsewhere. We will order these constraints in A in “row-major” order: recalling that $i \neq j$, this means we have first $i = 1 \ j = 2$, then $i = 1 \ j = 3$,

up to $i = 1$ $j = N$, followed by $i = 2$ $j = 1$, $i = 2$ $j = 3$, and so on. Let $\ell(i, j)$ give the index of the corresponding constraint, so that e.g. $\ell(1, 3) = 2$.

Now, the problem can be written

$$\min_{\mathbf{w} \in \mathbb{R}^{Nd}} \frac{1}{2} \|\mathbf{w}\|^2 \text{ s.t. } A\mathbf{w} + \mathbf{1} \leq \mathbf{0},$$

with the $\frac{1}{2}$ introduced for convenience. The KKT conditions for this problem are

$$\mathbf{w} + A^\top \mu = \mathbf{0} \quad A\mathbf{w} + \mathbf{1} \leq \mathbf{0} \quad \mu \geq \mathbf{0} \quad \mu \odot (A\mathbf{w} + \mathbf{1}) = \mathbf{0},$$

where \odot is elementwise multiplication. From the first condition, $\mathbf{w} = -A^\top \mu$, where $\mu \in \mathbb{R}^{N(N-1)}$ is any vector satisfying

$$\mu \geq \mathbf{0} \quad AA^\top \mu - \mathbf{1} \geq \mathbf{0} \quad \mu \odot (AA^\top \mu - \mathbf{1}) = \mathbf{0}.$$

Since (6) is a strictly convex minimization problem with affine constraints, these conditions are necessary and sufficient for optimality, and the solution \mathbf{w} is unique.

We can reasonably expect, since the x_i are orthonormal, that all constraints should be active, meaning that $AA^\top \mu = \mathbf{1}$. Indeed, choosing $\mu = (AA^\top)^{-1} \mathbf{1}$ automatically satisfies the second and third conditions; it only remains to show that this $\mu \geq \mathbf{0}$ in order to show this as an optimal solution to (6).

To do this, we will explicitly characterize AA^\top :

$$(AA^\top)_{\ell(i,j), \ell(i',j')} = x_i^\top (E_j - E_i)^\top (E_{j'} - E_{i'}) x_{i'} = (\delta_{ii'} + \delta_{jj'} - \delta_{ij'} - \delta_{ji'}) x_i^\top x_{i'},$$

where $\delta_{ij} = \mathbf{1}(i = j)$ is the Kronecker delta, since $E_i^\top E_j = \delta_{ij} I_d$.

Since the x_i are orthonormal, $x_i^\top x_{i'} = \delta_{ii'}$. As we know $i \neq j$ and $i' \neq j'$, this simplifies to

$$(AA^\top)_{\ell(i,j), \ell(i',j')} = \delta_{ii'} (1 + \delta_{jj'}).$$

Thus (AA^\top) is a block matrix with diagonal blocks of size $(N-1) \times (N-1)$ with values $I_{N-1} + \mathbf{1}_{N-1} \mathbf{1}_{N-1}^\top$, and all off-diagonal blocks zero. Taking $\mu = (AA^\top)^{-1} \mathbf{1}_{N(N-1)}$, the zero blocks contribute nothing, so each block of $N-1$ entries of μ is $(I_{N-1} + \mathbf{1}_{N-1} \mathbf{1}_{N-1}^\top)^{-1} \mathbf{1}_{N-1}$.

Note that $\mathbf{1}_{N-1} \mathbf{1}_{N-1}^\top$ has one eigenvector $v_1 = \frac{1}{\sqrt{N-1}} \mathbf{1}$ with eigenvalue $\lambda_1 = N-1$, and the remaining eigenvalues are all zero with eigenvectors satisfying $v_i^\top \mathbf{1} = 0$. Adding I to this matrix simply increases all eigenvalues by one. Thus,

$$(I + \mathbf{1} \mathbf{1}^\top)^{-1} \mathbf{1} = \frac{1}{N} \left(\frac{1}{\sqrt{N-1}} \mathbf{1} \right) \left(\frac{1}{\sqrt{N-1}} \mathbf{1} \right)^\top \mathbf{1} \quad (7)$$

$$+ \sum_{i=2}^{N-1} v_i \underbrace{v_i^\top \mathbf{1}}_0 = \frac{1}{N} \underbrace{\mathbf{1}^\top \mathbf{1}}_1 \mathbf{1} = \frac{1}{N} \mathbf{1}, \quad (8)$$

and so $\mu = \frac{1}{N} \mathbf{1}_{N(N-1)}$, which is indeed $\geq \mathbf{0}$; thus this is an optimal solution to the problem.

We next reconstruct $\mathbf{w} = -A^\top \mu = -\frac{1}{N} A^\top \mathbf{1}_{N(N-1)}$. Consider the block w_i inside \mathbf{w} ; its value will be the negative mean of the entries of A with an E_i in them. The $\ell(i, j)$ rows for $j \neq i$ contribute $N - 1$ entries of the form $-E_i x_i$. We also have the $\ell(k, i)$ rows, which have one $E_i x_k$ term for each $k \neq i$. Thus

$$w_i = -\frac{1}{N} \left(-(N-1)x_i + \sum_{k \neq i} x_k \right) = -\frac{1}{N} \left(-Nx_i + \sum_{k=1}^N x_k \right) = x_i - \bar{x},$$

where $\bar{x} = \frac{1}{N} \sum_{k=1}^N x_k$. Thus, for a test point x ,

$$\arg \max_i w_i^\top x = \arg \max_i x_i^\top x - \bar{x}^\top x = \arg \max_i x_i^\top x.$$

Because the x_i are orthonormal, this is further equal to

$$\arg \min_i \|x_i\|^2 + \|x\|^2 - 2x_i^\top x = \arg \min_i \|x - x_i\|. \quad \square$$

Lemma 1. *If $X \mid Y = y \sim \mathcal{N}(\mu_y, \sigma^2 I)$ and $Y \sim \text{Uniform}([N])$, the Bayes-optimal classifier is given by*

$$f^*(x) = \arg \min_y \|x - \mu_y\|.$$

Proof. This well-known fact follows by combining

$$p(Y = y \mid X = x) = \frac{p(X = x \mid Y = y)p(Y = y)}{p(X = x)} \propto p(X = x \mid Y = y)$$

with the definition of the density for X ,

$$\arg \max_y \frac{1}{(2\pi\sigma^2)^{d/2}} \exp \left(-\frac{1}{2\sigma^2} \|x - \mu_y\|^2 \right) = \arg \min_y \|x - \mu_y\|. \quad \square$$

B Implementation Details for Meta Learning Algorithms

Metric-based We use a meta learning library called learn2learn [5] to implement **ProtoNet** [61]. Following the original paper, we train a model with 30-way and 20-way for 1-Shot and 5-Shot, respectively, for 3,000 iterations. We use a 4 layer convolutional neural network (Conv4) with 64 channel size, and the batch size is set to 100. For optimization, we employ an Adam optimizer with a learning rate of 0.01 without having a learning rate schedule.

Optimization-based We use learn2learn library to implement both **MAML** [17] and **ANIL** [51]. We use Conv4 with 32 channel size for MAML and 64 channel size for ANIL (larger channel size does not perform better for MAML). We train both MAML and ANIL for 60,000 iterations. For optimizer, we employ an Adam optimizer for both with learning rates of 0.003 and 0.001 (adaptation

learning rates of 0.5 and 0.1) for MAML and ANIL, respectively. Batch sizes are set to 32 for both.

For **MetaOptNet** [40], we use the publicly available code provided by the authors of the paper (<https://github.com/kjunelee/MetaOptNet>). We employ the dual formulation of Support Vector Machine (SVM) proposed in MetaOptNet (MetaOptNet-SVM) for experiments with the training shot of 15, and use the default hyperparameter settings. For instance, we use a SGD optimizer with initial learning rate of 0.1 which decays step-wise. We train a model for 60 epochs with a batch size of 8.

Model-based For both Conditional Neural Process (CNP) [20] and Attentive Neural Process (ANP) [35], we use the publicly available code provided by the authors of the paper that addresses regression tasks for computer vision problems [19] (<https://github.com/boschresearch/what-matters-for-meta-learning>).

As the authors provide the model checkpoints for CNP on Distractor dataset and ANP on ShapeNet1D, we utilize them to compare active learning methods in meta-test time. We use 2-Shot for context sets in meta-test time instead of 25-Shot as done in the original work, since 25-Shot is too large to investigate the difference between active learning methods.

Pre-training-based We use the publicly available code provided by the authors of the papers for both **Baseline++** [12] (<https://github.com/wyharveychen/CloserLookFewShot>) and **SimpleShot** [68] (https://github.com/mileyan/simple_shot). For both models, we use the features from the pre-trained models on the whole training dataset in inference time. As reported in the public repository for Baseline++, the performance on CUB for 1-Shot and 5-Shot is lower than the numbers reported in the paper by about 1.1% and 2.5%, respectively. Similarly, the reproduced performance of SimpleShot for 1-Shot and 5-Shot is lower by about 4 ~ 5%. Note that the numbers correspond for the case of fully stratified random sampling.

C Relationship with Semi-Supervised Few-Shot learning

In this section, we describe the relationship between active meta-learning and semi-supervised few-shot learning [53, 69].

Both semi-supervised few-shot learning and active meta-learning aim to reduce the cost of manual data annotation, but they approach this goal differently. Semi-supervised few-shot learning leverages unlabeled data points without additional annotation, while active meta-learning iteratively adds new labeled data points selected from an unlabeled pool.

Among semi-supervised few-shot learning approaches, pseudo-labeling [31] is particularly closely related to active learning. Both pseudo-labeling and active learning utilize unlabeled data, but their methodologies differ. Active learning

uses uncertainty or diversity to select data for oracle labeling, targeting points whose labels are unknown. In contrast, pseudo-labeling uses a trained model to predict data labels, which can introduce errors if predictions are incorrect. Thus, pseudo-labeling focuses on data points where the model is already confident—precisely the points active learning would not select.

Combining these contrasting methods could be beneficial and interesting. Pseudo-labeling requires a well-trained classifier, which active learning can support by providing a robust labeled dataset.

D Implementation Details for Active Learning Strategies

In this section, we provide detailed description for the implementation of the following active learning methods.

DPP [8] We use DPPy library [23] to implement DPP selection. Gram matrix of the features from the penultimate layer are used as L-ensembles for DPP. We employ k -DPP to select k number of context data points.

Coreset [57] We refer to both original code and code provided by the authors of Typiclust and ProbCover. Since we assume that there is no initial labeled data points, we randomly choose the first data point and then apply the greedy algorithm after that.

Typiclust [27] We refer to the publicly available code provided by the authors of the paper (<https://github.com/avihu111/TypiClust>). As the maximum number of data points to annotate is 25 ($= 5\text{-Way} \times 5\text{-Shot}$), we do not set the maximum number of clusters unlike the original paper. We set the k in k -NN to 20 as with the original work.

ProbCover [70] We use the code provided by the original authors of the paper (it is the same as Typiclust). As we state in Appendix G and Appendix J, we exploit the features from the meta learners instead of self-supervised features to determine the radius parameters of ProbCover. In particular, the radius for each algorithm and dataset combination is determined as shown in Appendix G.

GMM (Ours) We refer to a publicly available implementation for GMM (<https://github.com/ldeেকে/gmm-torch>). As previously mentioned, we initialize the cluster centers using k -means. Then, we update the cluster means and covariance matrix (shared by all the clusters) using expectation maximization algorithm for up to 100 iterations. We make the covariance matrix shared between the clusters because we assume that the “influence” of each annotated data point to other data points is roughly the same regardless of data point although the weight of each dimension may be different (if they are the same, it is equivalent to k -means).

E Comparison of quality of selected data points

In this section, we estimate the quality of selected data points from the low budget active learning methods. In Fig. 5, we compare them in the distance and

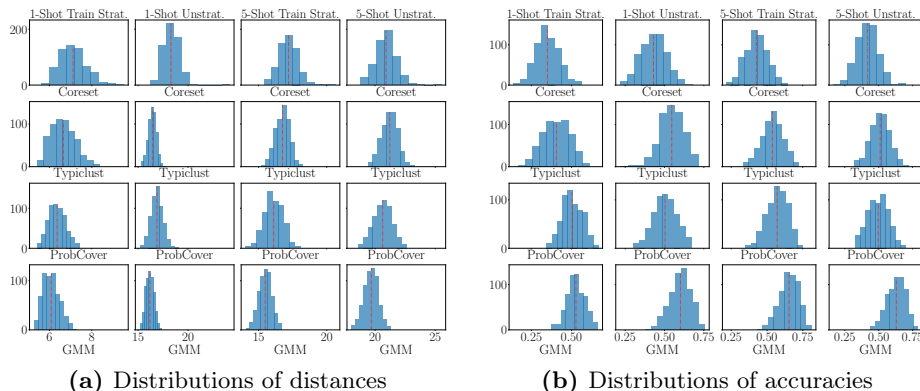


Fig. 5: Estimation of goodness of selected data points on MiniImageNet with ANIL using the distribution of (a) the distance between the unlabeled points and closest selected points, and (b) the equality between the true labels of unlabeled points and labels of the closest select points. Red dotted lines show mean values.

Data & Model	Clustering	1-Shot			5-Shot		
		Fully strat.	Train strat.	Unstrat.	Fully strat.	Train strat.	Unstrat.
MiniImage. MAML	<i>k</i> -means	56.75 ± 0.20	33.29 ± 0.26	37.26 ± 0.18	65.76 ± 0.18	41.61 ± 0.24	59.17 ± 0.20
	<i>k</i> -means++	56.12 ± 0.26	32.87 ± 0.32	38.53 ± 0.21	65.49 ± 0.21	43.61 ± 0.32	58.63 ± 0.26
	GMM	58.82 ± 0.24	33.34 ± 0.24	37.68 ± 0.19	67.18 ± 0.18	54.35 ± 0.20	59.05 ± 0.20
FC100 ProtoNet	<i>k</i> -means	50.20 ± 0.17	29.69 ± 0.20	35.03 ± 0.23	54.07 ± 0.17	41.42 ± 0.23	41.34 ± 0.23
	<i>k</i> -means++	49.91 ± 0.17	27.27 ± 0.22	34.93 ± 0.27	54.72 ± 0.30	41.61 ± 0.39	42.64 ± 0.39
	GMM	50.22 ± 0.18	34.23 ± 0.23	35.03 ± 0.23	54.76 ± 0.17	46.30 ± 0.21	47.03 ± 0.20

Table 7: Comparison of GMM and *k*-Means selections on MiniImageNet and FC100 using MAML and ProtoNet.

accuracy as explained in the caption with ANIL [51] on MiniImageNet. Whether a task is 1-Shot or 5-Shot, or train-time stratified or unstratified, we can observe that the metrics for GMM are consistently the best.

F Comparison to *k*-Means based methods

Tab. 7 compares the proposed GMM method to *k*-means and *k*-means++ since they are closely related.

The performance of GMM, *k*-means and *k*-means++ are similar in general but for some cases, GMM is significantly better than the others. We conjecture it is because some features are more important than the others, and since GMM takes it into account using Mahalanobis distance (instead of Euclidean distance used in *k*-means), it selects data points that represents nearby data points better.

G Difficulty of Tuning δ Parameter for ProbCover

In Section 3.2 of Yehuda *et al.* [70], the authors proposed to tune the radius δ based on the purity defined as,

$$\pi(\delta) = P(\{x : B_\delta(x) \text{ is pure}\}) \quad \text{where} \quad B_\delta(x) = \{x' : \|x' - x\|_2 \leq \delta\} \quad (9)$$

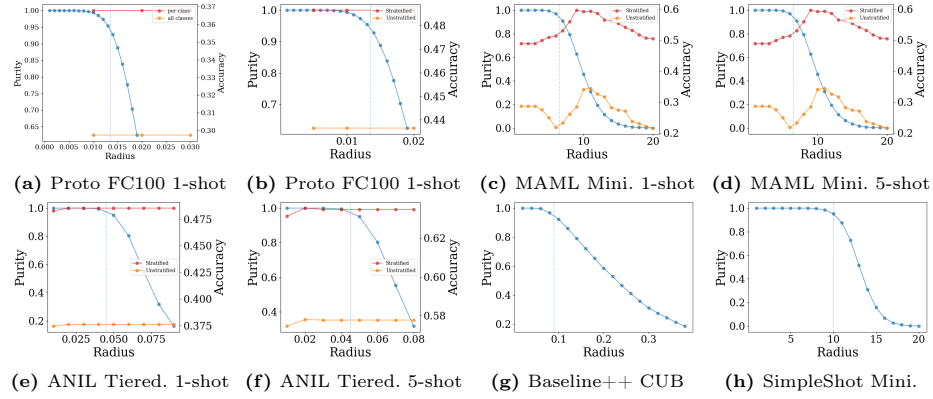


Fig. 6: Estimation of the optimal radius for ProbCover in meta-learning

Here, a ball $B_\delta(x)$ is “pure” if $f(x') = y, \forall x' \in B_\delta(x)$ where y is the label of x . As the radius δ increases, the purity decreases monotonically. They choose the optimal radius δ^* as $\delta^* = \max\{\delta : \pi(\delta) \geq 0.95\}$. More specifically, they first run k-means with k being the number of classes. Then, the purity is measured using the k-means assignment as pseudo-labels.

In their setting (pool-based active learning for image classification), since it is hard to obtain meaningful features from a model trained only a few examples, they use the features from self-supervised learning methods such as SimCLR [11]. It is, however, not the case for meta-learning. In meta-test time, the features from the meta learner are usually more meaningful than self-supervised learning features. Hence, we use the meta learner’s features to estimate the optimal radius for ProbCover. Following the original paper, we first run k-means and compute the purity in the same way. Since the features can differ by meta learning algorithms and the number of shots, we provide the plots for different algorithms as well as 1 and 5-Shots as shown in Fig. 6 (we select the optimal radius δ based on these plots throughout the experiments). For Fig. 6(a)-(f), we also provide the meta-test performance of stratified and unstratified versions of Random selection to demonstrate that the estimated optimal radius and best radius for meta-test accuracy do not align.

Another difficulty of estimating the optimal radius is that it is hard to set a search space for the radius. As shown in the x-axis of Fig. 6, the reasonable search space varies significantly depending on the meta-learning algorithms and datasets we use. In Yehuda *et al.*, this was less of a problem since they use SimCLR features, which are normalized: the range of the radius is in $[0, 1]$. However, as shown in Appendix J, if we use SimCLR features in meta-test time to actively select context sets, the performance generally drops.

H Additional Experimental Results for Classification

In this section, we provide additional experimental results for few-shot image classification. In Tab. 8, we compare the active learning strategies for ANIL [51]

$\text{Pick}_\theta^{\text{eval}}$	1-Shot			5-Shot		
	Fully strat.	Train strat.	Unstrat.	Fully strat.	Train strat.	Unstrat.
Random	47.55 \pm 0.18	38.19 \pm 0.16	34.79 \pm 0.15	63.84 \pm 0.17	57.92 \pm 0.23	57.56 \pm 0.18
Entropy	43.89 \pm 0.16	32.73 \pm 0.16	26.33 \pm 0.14	57.56 \pm 0.18	40.23 \pm 0.18	34.16 \pm 0.17
Margin	47.35 \pm 0.17	36.01 \pm 0.14	30.79 \pm 0.14	62.87 \pm 0.17	54.89 \pm 0.24	56.76 \pm 0.17
DPP	49.28 \pm 0.17	38.17 \pm 0.15	36.52 \pm 0.15	63.24 \pm 0.19	57.28 \pm 0.21	57.23 \pm 0.18
Coreset	47.32 \pm 0.18	36.97 \pm 0.20	40.72 \pm 0.14	56.93 \pm 0.18	47.68 \pm 0.22	52.89 \pm 0.17
Typiclust	52.95 \pm 0.18	37.21 \pm 0.17	34.05 \pm 0.14	63.13 \pm 0.19	55.84 \pm 0.22	56.76 \pm 0.17
ProbCover	48.53 \pm 0.53	37.61 \pm 0.49	34.53 \pm 0.43	63.48 \pm 0.51	57.77 \pm 0.56	57.12 \pm 0.58
GMM (Ours)	60.29 \pm 0.19	50.92 \pm 0.22	42.17 \pm 0.17	66.48 \pm 0.18	60.12 \pm 0.24	60.28 \pm 0.17

Table 8: 5-Way K-Shot on TieredImageNet with ANIL, with $\text{Pick}_\theta^{\text{train}}$ random.

$\text{Pick}_\theta^{\text{eval}}$	1-Shot			5-Shot		
	Fully strat.	Train strat.	Unstrat.	Fully strat.	Train strat.	Unstrat.
Random	40.41 \pm 0.74	31.96 \pm 0.56	32.76 \pm 0.63	53.11 \pm 0.66	47.73 \pm 0.70	47.48 \pm 0.76
DPP	40.47 \pm 0.80	30.33 \pm 0.67	33.41 \pm 0.66	51.44 \pm 0.68	48.21 \pm 0.67	47.45 \pm 0.68
Coreset	39.20 \pm 0.71	27.55 \pm 0.66	30.16 \pm 0.69	46.80 \pm 0.67	24.08 \pm 0.65	25.75 \pm 0.72
Typiclust	45.20 \pm 0.78	26.35 \pm 0.47	27.00 \pm 0.43	52.39 \pm 0.66	23.97 \pm 0.42	24.12 \pm 0.39
ProbCover	41.93 \pm 0.67	26.87 \pm 0.62	27.43 \pm 0.48	54.36 \pm 0.76	37.00 \pm 0.69	38.33 \pm 0.76
GMM (Ours)	51.16 \pm 0.67	40.89 \pm 0.74	41.61 \pm 0.87	60.48 \pm 0.86	52.68 \pm 0.70	51.79 \pm 0.70

Table 9: 5-Way K-Shot on FC100 with MetaOptNet, with $\text{Pick}_\theta^{\text{train}}$ random.

$\text{Pick}_\theta^{\text{eval}}$	1-Shot		5-Shot	
	Fully strat.	Train strat.	Fully strat.	Train strat.
Random	45.15 \pm 0.73	26.28 \pm 0.61	61.22 \pm 0.72	51.89 \pm 0.73
Entropy	37.08 \pm 0.75	21.62 \pm 0.37	47.93 \pm 0.74	32.74 \pm 0.60
Margin	41.53 \pm 0.73	24.28 \pm 0.51	62.15 \pm 0.70	50.90 \pm 0.75
DPP	44.52 \pm 0.75	26.32 \pm 0.58	60.93 \pm 0.72	51.79 \pm 0.75
Coreset	45.85 \pm 0.73	27.04 \pm 0.54	56.48 \pm 0.72	40.39 \pm 0.68
Typiclust	44.53 \pm 0.71	22.97 \pm 0.42	34.21 \pm 0.77	20.04 \pm 0.06
ProbCover	49.32 \pm 0.71	24.61 \pm 0.52	55.60 \pm 0.66	32.24 \pm 0.67
GMM (Ours)	52.77 \pm 0.72	28.17 \pm 0.64	62.64 \pm 0.71	50.40 \pm 0.75

Table 10: 5-Way K-Shot on MiniImageNet with SimpleShot, with $\text{Pick}_\theta^{\text{train}}$ random.

on the TieredImageNet dataset. Similarly, Tab. 9 provides the results with MetaOptNet [40] on FC100 dataset. Tab. 10, Tab. 11, and Tab. 12 are for SimpleShot [68], ProtoNet [61], and ANIL [51] on MiniImageNet, respectively. Note that Entropy and Margin selections are not applicable for MetaOptNet-SVM. Regardless of meta-learning algorithm and dataset, GMM significantly outperforms the other active learning methods, and some of them are worse than the Random selection.

I Additional Experimental Details for Regression

Gao *et al.* propose the Distractor and ShapeNet1D datasets to compare meta learning algorithms for vision regression tasks. They evaluate meta learners for

$\text{Pick}_\theta^{\text{eval}}$	1-Shot			5-Shot		
	Fully strat.	Train strat.	Unstrat.	Fully strat.	Train strat.	Unstrat.
Random	47.70 \pm 0.20	39.65 \pm 0.28	38.72 \pm 0.27	64.66 \pm 0.18	57.36 \pm 0.27	57.42 \pm 0.25
Entropy	44.33 \pm 0.20	36.35 \pm 0.28	34.87 \pm 0.27	61.23 \pm 0.19	49.83 \pm 0.31	48.46 \pm 0.32
Margin	47.07 \pm 0.20	37.69 \pm 0.27	37.84 \pm 0.28	63.79 \pm 0.18	55.25 \pm 0.29	56.15 \pm 0.27
DPP	47.90 \pm 0.20	39.17 \pm 0.28	37.89 \pm 0.26	64.36 \pm 0.19	57.48 \pm 0.26	57.37 \pm 0.25
Coreset	47.86 \pm 0.20	39.51 \pm 0.26	37.79 \pm 0.26	55.09 \pm 0.20	50.14 \pm 0.29	50.27 \pm 0.28
Typiclust	59.51 \pm 0.17	38.47 \pm 0.27	37.57 \pm 0.27	61.02 \pm 0.19	51.82 \pm 0.31	52.02 \pm 0.30
ProbCover	48.51 \pm 0.20	35.25 \pm 0.26	34.50 \pm 0.25	43.61 \pm 0.19	38.63 \pm 0.21	38.24 \pm 0.20
GMM (Ours)	64.50 \pm 0.16	47.88 \pm 0.32	44.71 \pm 0.29	67.03 \pm 0.19	57.55 \pm 0.29	56.44 \pm 0.30

Table 11: 5-Way K-Shot on MiniImageNet with ProtoNet, with $\text{Pick}_\theta^{\text{train}}$ random.

$\text{Pick}_\theta^{\text{eval}}$	1-Shot			5-Shot		
	Fully strat.	Train strat.	Unstrat.	Fully strat.	Train strat.	Unstrat.
Random	46.59 \pm 0.19	36.70 \pm 0.19	34.79 \pm 0.18	61.35 \pm 0.19	55.24 \pm 0.20	56.65 \pm 0.19
Entropy	44.63 \pm 0.20	35.51 \pm 0.18	27.35 \pm 0.14	55.09 \pm 0.19	39.71 \pm 0.20	37.45 \pm 0.19
Margin	46.58 \pm 0.19	36.60 \pm 0.19	32.46 \pm 0.18	55.62 \pm 0.19	40.40 \pm 0.20	37.67 \pm 0.19
DPP	47.33 \pm 0.19	37.45 \pm 0.17	37.76 \pm 0.18	61.08 \pm 0.19	56.18 \pm 0.18	57.08 \pm 0.18
Coreset	46.40 \pm 0.21	38.37 \pm 0.17	41.34 \pm 0.17	53.74 \pm 0.20	47.81 \pm 0.20	51.62 \pm 0.19
Typiclust	54.44 \pm 0.18	36.78 \pm 0.17	34.52 \pm 0.19	60.87 \pm 0.18	52.56 \pm 0.20	55.11 \pm 0.19
ProbCover	51.56 \pm 0.18	27.49 \pm 0.15	41.46 \pm 0.17	61.68 \pm 0.18	53.80 \pm 0.20	42.70 \pm 0.22
GMM (Ours)	58.50 \pm 0.18	48.13 \pm 0.20	40.26 \pm 0.18	65.14 \pm 0.17	59.01 \pm 0.20	61.48 \pm 0.19

Table 12: 5-Way K-Shot on MiniImageNet with ANIL, with $\text{Pick}_\theta^{\text{train}}$ random.

intra-category (IC) and cross-category (CC) inputs where CC corresponds to the cross-domain in few-shot image classification.

Distractor consists of 10 object classes for a training set and 2 novel classes for CC evaluation. Each class contains 1,000 randomly sampled objects from ShapeNetCoreV2 [10]. 20% of training set is reserved for IC evaluation. In this dataset, each image consists of two objects: the object of interest and a distractor object, which are positioned randomly. The goal is to recognize and locate the object of interest within the image in the presence of a distractor.

ShapeNet1D [19] consists of 27 object classes for a training set and 3 object classes for CC evaluation. Each object class contains 50 images, and 10 images are used for IC evaluation. ShapeNet1D aims to predict the 1D pose, i.e., rotation angle, around the azimuth axis of an object.

To analyze these vision regression tasks, we compare various active learning strategies in the 2-shot setting. We use CNP for Distractor, NP for ShapeNet1D. More details about the models can be found in Appendix B.

J Comparison to Self-Supervised Features

ProbCover and Typiclust use self-supervised features to actively select new data points to annotate, since there are not enough labeled data to train a classifier to output meaningful features. Instead, they utilize the features from SimCLR [11]. To validate if it is better to use the features from a meta learner than SimCLR in

Dataset	Features	1-Shot			5-Shot		
		Fully strat.	Train strat.	Unstrat.	Fully strat.	Train strat.	Unstrat.
Mini.	MAML	55.65 \pm 0.18	27.45 \pm 0.17	35.46 \pm 0.18	64.16 \pm 0.18	46.70 \pm 0.21	57.83 \pm 0.21
	SimCLR	44.84 \pm 0.44	27.59 \pm 0.35	34.80 \pm 0.47	65.95 \pm 0.43	36.03 \pm 0.48	57.77 \pm 0.47
FC100	ProtoNet	46.01 \pm 0.16	30.96 \pm 0.19	30.61 \pm 0.21	47.54 \pm 0.17	43.61 \pm 0.18	44.03 \pm 0.21
	SimCLR	36.07 \pm 0.44	29.60 \pm 0.46	30.13 \pm 0.45	48.59 \pm 0.49	43.29 \pm 0.49	43.89 \pm 0.59

Table 13: Comparison of MAML and SimCLR features for Typiclust.

Dataset	Features	1-Shot			5-Shot		
		Fully strat.	Train strat.	Unstrat.	Fully strat.	Train strat.	Unstrat.
Mini.	MAML	52.81 \pm 1.16	21.91 \pm 0.24	36.21 \pm 0.18	64.70 \pm 0.91	42.07 \pm 0.49	23.40 \pm 0.36
	SimCLR	47.57 \pm 0.42	25.35 \pm 0.38	32.19 \pm 0.43	64.33 \pm 0.39	36.64 \pm 0.58	26.16 \pm 0.43
FC100	ProtoNet	48.66 \pm 0.16	32.86 \pm 0.22	33.58 \pm 0.19	51.11 \pm 0.17	44.20 \pm 0.24	44.40 \pm 0.24
	SimCLR	31.40 \pm 0.42	29.53 \pm 0.42	28.39 \pm 0.43	47.11 \pm 0.39	39.33 \pm 0.54	45.40 \pm 0.52

Table 14: Comparison of MAML and SimCLR features for ProbCover.

meta-learning, we compare SimCLR features to the features from either MAML or ProtoNet for Typiclust and ProbCover as shown in Tab. 13 and Tab. 14. Here, we use MiniImageNet and FC100 datasets for MAML and ProtoNet, respectively as with Tab. 2 and Tab. 1. For both Typiclust and ProbCover, although there are a couple of cases where SimCLR features are better, it is significantly worse than MAML and ProtoNet features in general. It intuitively makes sense because 1) meta learners are trained with large enough data points and 2) it is likely that the information in self-supervised features do not align with that in meta learners.

K Sequential Active-Meta Learning

Although iterative sampling is more common in active learning, we have focused on sampling a context set at once because of the following two reasons.

First, even though we iterative label additional samples, the features do not change in most of meta-learning algorithms except for MAML. Even for other optimization-based methods such as ANIL, since the feature extractor is not updated during adaptation on a context set, the features will stay the same for iterative process of active learning. As we demonstrated with ProtoNet in Fig. 7 (c)-(d) (details about experiments are below), although we iteratively add more labeled samples, the performance does not change much as the features do not change. In this case, selecting $N \times K$ samples at once is not different from iterative process while it is cheaper.

Furthermore, if we iteratively add labeled samples, it will quickly go beyond few-shot regime in meta-learning, which is often not that practical in real world settings. Suppose we have a meta learner trained in 5-way 1-Shot. It is reasonable to add 5 samples per iteration since it is the minimum number to cover all the classes. But only after 5 iterations, it will go few-shot regime where we typically have 25 labeled context samples. It is even less practical for 5-Shot case.

Fig. 7 compare active learning methods for sequential setting where we select 5 context samples at a time until the budget reaches 25 samples. Every

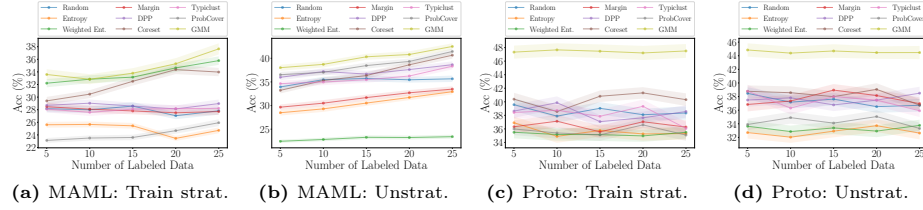


Fig. 7: Test performance of MAML and ProtoNet on MiniImageNet with sequentially actively selected context sets. 5 context samples are selected at each iteration until it reaches 25.

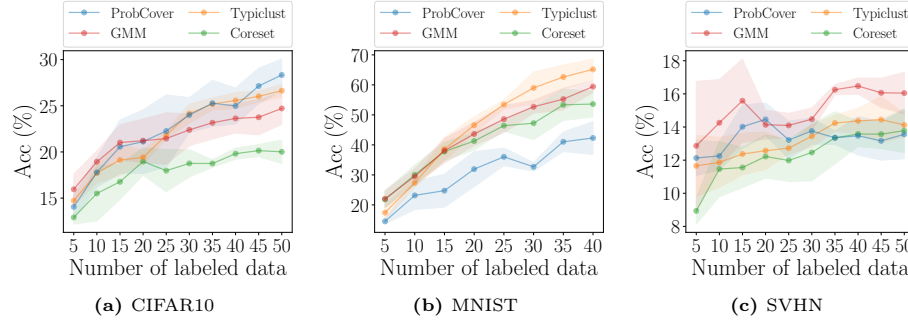


Fig. 8: Low-budget active learning methods on image classification with very low budget. Mean and standard error of accuracy for three sets of SimCLR features, three runs per features.

time we select new context samples we may utilize them to maximize new label information. For MAML, we update all the model parameters through adaptation steps. It is, however, not applicable to the other meta-learning methods we use in this work including ProtoNet, since none of the other methods including optimization-based methods such as ANIL, do not update the parameters up to the penultimate layer.

As expected, the test performance of ProtoNet does not change much regardless of active learning methods. But, the test performance of MAML gradually increases as we add more context samples. In sequential active-meta learning, GMM still significantly outperforms other active learning methods.

L Fitting GMM using Expectation Maximization

In this section, we provide details about fitting GMM using the expectation maximization (EM) algorithm. Although it is available in many literature, we add it here for completeness of our method. The log-likelihood objective for a

GMM is given by,

$$\ell(\theta) = \sum_{i=1}^N \log \left(\sum_{k=1}^K \pi_k \mathcal{N}(x_i | \mu_k, \Sigma_k) \right), \quad (10)$$

where model parameters $\theta = \{(\pi_k, \mu_k, \Sigma_k)\}_{k=1}^K$ with N and K being the number of samples and mixture components, respectively.

EM algorithm is an iterative algorithm where we alternatively conduct E-step and M-step as follows,

- E-step: we compute the posterior probability w_{ik} that represents i -th data point belongs to the k -th Gaussian component as,

$$w_{ik} = \frac{\pi_k \mathcal{N}(x_i | \mu_k, \Sigma_k)}{\sum_{j=1}^K \pi_j \mathcal{N}(x_i | \mu_j, \Sigma_j)} \quad (11)$$

- M-step: we maximize the log-likelihood in terms of the model parameters. Fortunately, for GMM, there are closed form solutions for each parameter.

$$\pi_k = \frac{1}{N} \sum_{i=1}^N w_{ik}, \quad \mu_k = \frac{\sum_{i=1}^N w_{ik} x_i}{\sum_{i=1}^N w_{ik}}, \quad \Sigma_k = \frac{\sum_{i=1}^N w_{ik} (x_i - \mu_k)(x_i - \mu_k)^T}{\sum_{i=1}^N w_{ik}} \quad (12)$$

We repeat the E-step and M-step until convergence of the log-likelihood or for a fixed number of iteration time. Please note that we use diagonal covariance Σ_k since it is computationally efficient and often fits better in term of log-likelihood.

M Analysis on Low Budget Active Learning Methods

We briefly explain why each active learning method does not perform as well as the proposed GMM method or even Random selection. In this section, we discuss further on the inferiority of low budget active learning methods compared to GMM. We conjecture it may be attributed to its implicit exploration of locally dense regions or inappropriate measure of representativeness. Here we analyzed potential reasons of their failure in very low budget regime.

- Typiclust: after conducting k -means, it selects samples for each cluster j , based on

$$\arg \max_{x \in \text{clust}_j} \left(\frac{1}{K} \sum_{x_i \in \text{KNN}(x)} \|x - x_i\|_2 \right)^{-1}$$

where KNN denotes k -nearest neighbors of which size is fixed to 20. This measure seeks for locally dense region by selecting samples that are close to its nearest neighbors.

- ProbCover: it greedily finds the maximally covering samples given a fixed radius. This greedy algorithm provide $(1 - \frac{1}{e})$ -approximation for the optimal solution but the gap with the optimal solution can be quite large. Also, the selection of the radius is hard as we discussed in Appendix G. When the radius is small, it tries to find samples that are in locally dense regions.
- DPP: it finds samples of which a kernel matrix (with a pre-defined kernel function) has the maximum determinant, which implicitly finds diverse samples. The determinant of a matrix, however, may not align with selecting maximum covering (or representative) samples. In particular, maximizing the determinant of the kernel matrix may lead to selecting samples far away from other samples.

Compared to these methods, GMM tries to find globally representative samples in non-greedy fashion (using expectation maximization). Also, its measure of covering other samples is in Mahalanobis distance, which intuitively makes more sense than the determinant of a kernel matrix as a measure. The proposed GMM method is also theoretically motivated by the Corollary 1, which says a classifier trained with the selected samples from GMM (cluster means) is a Bayes-optimal classifier under certain conditions.

N Training-Time Active Learning

As mentioned in Sec. 5, we observe that active learning methods do not significantly change the generalization performance of meta learners when applied in meta-train time, which aligns with observations from [46, 58]. To empirically demonstrate it, we apply several active learning methods without stratification in the meta-train time for ProtoNet on MiniImageNet. Fig. 9 shows among Random, DPP and GMM selections, one is not significantly better than another although the Entropy selection is significantly worse than them.

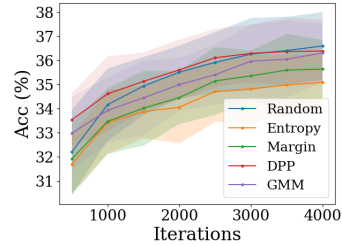


Fig. 9: Comparison of $\text{Pick}_{\theta}^{\text{train}}$.